

Numerical implementation of a VCSEL-based stochastic logic gate via polarization bistability

J. Zamora-Munt^{1,2} and C. Masoller^{1,3}

¹*Departament de Física i Enginyeria Nuclear, Universitat Politècnica de Catalunya, Colom 11, E-08222 Terrassa, Barcelona, Spain*

²*jordi.zamora.munt@upc.edu*

³*crisrina.masoller@upc.edu*

Abstract: We study the interplay of polarization bistability, spontaneous emission noise and aperiodic current modulation in vertical cavity surface emitting lasers (VCSELs). We demonstrate the phenomenon of logic stochastic resonance (LSR), by which the laser gives robust and reliable logic response to two logic inputs encoded in an aperiodic signal directly modulating the laser bias current. The probability of a correct response is controlled by the noise strength, and is equal to 1 in a wide region of noise strengths. LSR is associated with optimal noise-activated polarization switchings (the so-called “inter-well” dynamics if one considers the VCSEL as a bistable system described by a double-well potential) and optimal sensitivity to spontaneous emission in each polarization (the “intra-well” dynamics in the double-well potential picture). The robust nature of LSR in VCSELs offers interesting perspectives for novel applications and provides yet another example of a driven nonlinear optical system where noise can be employed constructively.

© 2010 Optical Society of America

OCIS codes: (250.7260) Vertical cavity surface emitting lasers; (140.3430) Laser theory.

References and links

1. F. Koyama, “Recent advances of VCSEL photonics,” *J. Lightwave Technol.* **24**, 4502–4513 (2006).
2. G. Giacomelli, F. Marin, M. Gabrysch, K. H. Gulden, and M. Moser, “Polarization competition and noise properties of VCSELs,” *Opt. Commun.* **146**, 136–140 (1998).
3. H. Li, A. Hohl, A. Gavrielides, H. Hou, and K. D. Choquette, “Stable polarization self-modulation in vertical-cavity surface-emitting lasers,” *Appl. Phys. Lett.* **72**, 2355–2357 (1998).
4. T. Ackemann and M. Sondermann, “Characteristics of polarization switching from the low to the high frequency mode in vertical-cavity surface-emitting lasers,” *Appl. Phys. Lett.* **78**, 3574–3576 (2001).
5. S. Bandyopadhyay, Y. Hong, P. S. Spencer, and K. A. Shore, “Experimental observation of anti-phase polarisation dynamics in VCSELs,” *Opt. Commun.* **202**, 145–154 (2002).
6. J. Danckaert, M. Peeters, C. Mirasso, M. San Miguel, G. Verschaffelt, J. Albert, B. Nagler, H. Unold, R. Michalzik, G. Giacomelli, and F. Marin, “Stochastic polarization switching dynamics in vertical-cavity surface-emitting lasers: theory and experiment,” *IEEE J. Sel. Top. Quantum Electron.* **10**, 911–917 (2004).
7. M. Sciamanna and K. Panajotov, “Route to polarization switching induced by optical injection in vertical-cavity surface-emitting lasers,” *Phys. Rev. A* **73**, 023811 (2006).
8. P. A. Porta, D. P. Curtin, and J. G. McInerney, “Laser Doppler velocimetry by optical self-mixing, in vertical-cavity surface-emitting lasers,” *IEEE Photon. Technol. Lett.* **14**, 1719–1721 (2002).
9. J. Albert, M. C. Soriano, I. Veretennicoff, K. Panajotov, J. Danckaert, P. A. Porta, D. P. Curtin, and J. G. McInerney, “Laser Doppler velocimetry with polarization-bistable VCSELs,” *IEEE J. Sel. Top. Quantum Electron.* **10**, 1006–1012 (2004).

10. T. Katayama, T. Ooi, and H. Kawaguchi, "Experimental demonstration of multi-bit optical buffer memory using 1.55- μm polarization bistable vertical-cavity surface-emitting lasers," *IEEE J. Quantum Electron.* **45**, 1495–1504 (2009).
11. H. Kawaguchi, "Polarization-bistable vertical-cavity surface-emitting lasers: application for optical bit memory," *Opt. Electron. Rev.* **17**, 265–274 (2009).
12. T. Mori, Y. Sato, and H. Kawaguchi, "10-Gb/s optical buffer memory using a polarization bistable VCSEL," *IEICE Trans. Electron. E* **92C**, 957–963 (2009).
13. K. Murali, S. Shina, W. L. Ditto, and A. R. Bulsara, "Reliable logic circuit elements that exploit nonlinearity in the presence of a noise floor," *Phys. Rev. Lett.* **102**, 104101 (2009).
14. K. Murali, I. Rajamohamed, S. Shina, W. L. Ditto, and A. R. Bulsara, "Realization of reliable and flexible logic gates using noisy nonlinear circuits," *Appl. Phys. Lett.* **95**, 194102 (2009).
15. L. Worschech, F. Hartmann, T. Y. Kim, S. Hofling, M. Kamp, A. Forchel, J. Ahopelto, I. Neri, A. Dari, and L. Gammaitoni, "Universal and reconfigurable logic gates in a compact three-terminal resonant tunneling diode," *Appl. Phys. Lett.* **96**, 042112 (2010).
16. J. Martin-Regalado, F. Prati, M. San Miguel, and N. B. Abraham, "Polarization properties of vertical-cavity surface-emitting lasers," *IEEE J. Quantum Electron.* **33**, 765–783 (1997).
17. M. B. Willemsen, M. U. F. Khalid, M. P. van Exter, and J. P. Woerdman, "Polarization switching of a vertical-cavity semiconductor laser as a Kramers hopping problem," *Phys. Rev. Lett.* **82**, 4815–4818 (1999).
18. P. Mandel, *Theoretical Problems in Cavity Nonlinear Optics*, (Cambridge University Press, Cambridge, England, 1997).
19. C. Masoller, M. S. Torre, and P. Mandel, "Influence of the injection current sweep rate on the polarization switching of vertical-cavity surface-emitting lasers," *J. Appl. Phys.* **99**, 026106 (2006).
20. J. Paul, C. Masoller, Y. Hong, P. S. Spencer, and K. A. Shore "Experimental study of polarization switching of vertical-cavity surface-emitting lasers as a dynamical bifurcation," *Opt. Lett.* **31**, 748–750 (2006).
21. L. Gammaitoni, P. Hänggi, P. Jung, and F. Marchesoni, "Stochastic resonance," *Rev. Mod. Phys.* **70**, 223–287 (1998).
22. C. Masoller and N. B. Abraham, "Low-frequency fluctuations in vertical-cavity surface-emitting semiconductor lasers with optical feedback," *Phys. Rev. A* **59**, 3021–3031 (1999).
23. S. Balle, E. Tolkachova, M. San Miguel, J. R. Tredicce, J. Martin-Regalado, and A. Gahl, "Mechanisms of polarization switching in single-transverse-mode vertical-cavity surface-emitting lasers: thermal shift and nonlinear semiconductor dynamics," *Opt. Lett.* **24**, 1121–1123 (1999).
24. G. Verschaffelt, J. Albert, I. Veretennicoff, J. Danckaert, S. Barbay, G. Giacomelli, and F. Marin, "Frequency response of current-driven polarization modulation in vertical-cavity surface-emitting lasers," *Appl. Phys. Lett.* **80**, 2248–2250 (2002).
25. C. Masoller and M. S. Torre, "Modeling thermal effects and polarization competition in vertical-cavity surface-emitting lasers," *Opt. Express* **16**, 21282–21296 (2008).
26. M. Borromeo and F. Marchesoni, "Asymmetric probability densities in symmetrically modulated bistable devices," *Phys. Rev. E* **71**, 031105 (2005).
27. S. Barbay, G. Giacomelli, and F. Marin, "Noise-assisted binary information transmission in vertical cavity surface emitting lasers," *Opt. Lett.* **25**, 1095–1097 (2000).
28. S. Barbay, G. Giacomelli, and F. Marin, "Noise-assisted transmission of binary information: theory and experiment," *Phys. Rev. E* **63**, 051110 (2001).
29. D. V. Dylov and J. W. Fleischer, "Nonlinear self-filtering of noisy images via dynamical stochastic resonance," *Nature Photon.* **4**, 323–328 (2010).

1. Introduction

The vertical-cavity surface-emitting laser (VCSEL) is a type of semiconductor laser that has many advantages which are desirable for communications and signal processing, as compared to conventional ("edge-emitting") devices [1]. VCSELs are more compact, have a lower threshold and a higher modulation bandwidth. However, because of their circular transverse geometry, polarization bistability often occurs, and VCSELs can either emit linearly polarized light (with the polarization direction along one of two orthogonal directions associated with crystalline or stress orientations, referred to as x and y), or display a variety of nonlinear phenomena including stochastic polarization switching, anti-correlated polarization coexistence and elliptical polarization [2–7]. These phenomena are often considered a drawback, degrading the laser performance; however, they can also be exploited for applications, such as polarization-bistable VCSELs for laser Doppler velocimetry [8, 9]. Recently, polarization-bistable VCSELs were used to built optical buffer memories, in which the bit state of the optical signal, "0" or "1",

is stored as a lasing linear polarization state (x or y). Kawaguchi and coworkers [10–12] have shown experimentally that the polarization state can be transferred from one VCSEL to another VCSEL that is optically connected in cascade, and constructed a 4-bit optical buffer memory by connecting in parallel two such sets of cascade-coupled VCSELS.

In this article we propose a novel method for exploiting polarization bistability in VCSELS, based on the interplay of nonlinearity, bistability and noise. Our work is motivated by a recent article by Murali *et al.* [13], who demonstrated that a two-state system with two adjustable thresholds, modeled by a 1D double-well potential, can act as a reliable and flexible logic gate in the presence of an appropriate amount of noise, a phenomenon which was referred to as *logical stochastic resonance* (LSR). LSR was also recently demonstrated in an electronic circuit [14] and in a resonant tunneling diode [15].

The polarization dynamics of VCSELS can be qualitatively well understood in the framework of the spin-flip model [16], which consist of a set of six ordinary differential equations describing the evolution of the real and imaginary parts of two complex optical fields (associated with two orthogonal polarizations) as well as two carrier densities with opposite spin. The predicted polarization behavior, and specifically, the stochastic polarization switching, agrees well with that expected for stochastic switching in a 1D double-well potential [17]. Therefore, one might expect to observe LSR in the polarization of VCSELS.

In this article we perform numerical simulations of the spin-flip model and show that VCSELS operating in polarization bistable regimes can display LSR, which can be used to realize VCSEL-based robust logic gates, that give a reliable logic response to two logic inputs, even in the presence of a significant amount of noise. The two logic inputs are encoded in a three-level aperiodic signal directly applied to the laser bias current. Exploiting polarization bistability, one can consider that the laser response is a logic 1 if one polarization is emitted (referred to as x), and a logic 0 if the orthogonal polarization is emitted (referred to as y). Then, the truth table of the fundamental logical operators AND and OR (and their negations, NAND and NOR) can be reproduced and we show that the probability of a correct response is equal to one in a wide range of noise strengths.

This article is organized as follows: Sec. 2 presents the model; in Sec. 3 we show how two logic inputs can be encoded in a three-level aperiodic signal applied directly to the laser bias current. Section 4 presents numerical results that demonstrate that a VCSEL can operate as a logic gate under a suitable amount of noise. Section 5 discusses the reliability of the logic gate. The influence of the success detection criterium, as well as of various model parameters is analyzed. Section 6 presents a summary of the results and the conclusions.

2. Model

The rate equations for the orthogonal linearly polarized slowly-varying complex amplitudes, E_x and E_y , the total carrier density, $N = N_+ + N_-$, and the carrier difference, $n = N_+ - N_-$ (N_+ and N_- being carrier populations with opposite spin) are [16]:

$$\begin{aligned} \frac{dE_{x,y}}{dt} &= k(1 + i\alpha)[(N - 1)E_{x,y} \pm inE_{y,x}] \mp (\gamma_a + i\gamma_p)E_{x,y} + \sqrt{\beta_{sp}\gamma_N N} \xi_{x,y}, \\ \frac{dN}{dt} &= \gamma_N[\mu(t) - N(1 + |E_x|^2 + |E_y|^2) - in(E_y E_x^* - E_x E_y^*)], \\ \frac{dn}{dt} &= -\gamma_s n - \gamma_N[n(|E_x|^2 + |E_y|^2) + iN(E_y E_x^* - E_x E_y^*)], \end{aligned}$$

where k is the field decay rate, γ_N is the decay rate of the total carrier population, γ_s is the spin-flip rate, α the linewidth enhancement factor, γ_a and γ_p are linear anisotropies representing dichroism and birefringence, and $\mu(t)$ is the injection current parameter normalized such that

the static cw threshold in the absence of anisotropies is at $\mu_{th,s} = 1$.

β_{sp} is the coefficient of spontaneous emissions, the spontaneous emission rate being $R_{sp} = 4\beta_{sp}\gamma_N N$ (i.e., the fraction of the spontaneously emitted photons that goes into the lasing mode), and $\xi_{x,y}$ are uncorrelated Gaussian white noises with zero mean and unit variance. Since we will consider the laser biased above threshold, where the carrier density is clamped, we will approximate $N \sim N_0 = 1$ and define the noise strength parameter as $D = \beta_{sp}\gamma_N N_0$.

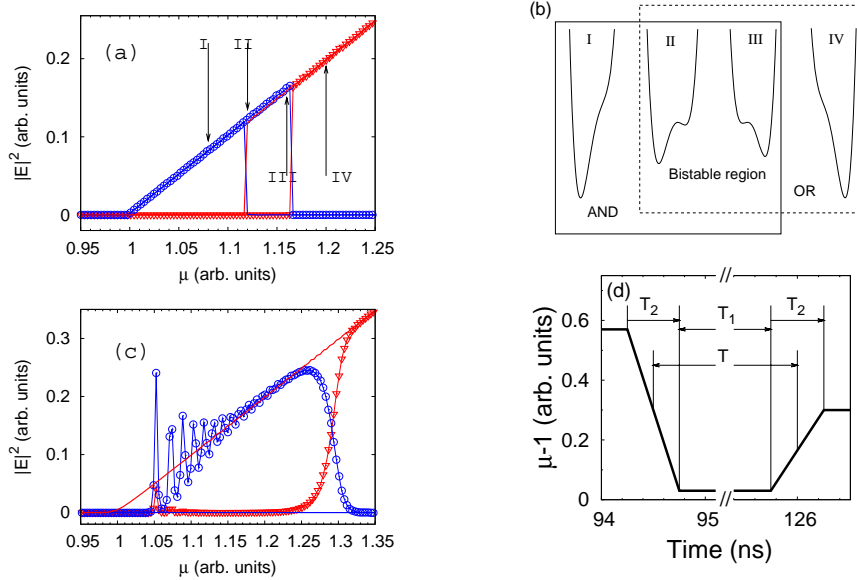


Fig. 1. (a) Intensities of the x and y polarizations when the injection current increases and decreases linearly, from $\mu_i = 0.95$ to $\mu_f = 1.4$ in a time interval equal to $40 \mu s$. x polarization in red for increasing (red triangles) and decreasing (red solid line) current; y polarization in blue for increasing (blue circles) and decreasing (blue solid line) current. The parameters are $k = 300 \text{ ns}^{-1}$, $\alpha = 3$, $\gamma_N = 1 \text{ ns}^{-1}$, $\gamma_a = 0.5 \text{ ns}^{-1}$, $\gamma_p = 50 \text{ rad ns}^{-1}$, $\gamma_s = 50 \text{ ns}^{-1}$ and $D = 10^{-6} \text{ ns}^{-1}$. (b) Schematic representation of the effective potential at four different pump current values, corresponding to labels I to IV in Fig. 1(a). The solid square indicates the three values that can be used for implementing a logic AND; the dashed square indicates the three values that can be used for implementing a logic OR (see text for details). (c) As Fig. 1(a) but when the injection current varies from $\mu_i = 0.95$ to $\mu_f = 1.4$ in a time interval equal to 25 ns . (d) Schematic representation of the current variation within a bit (see text for details).

The steady-state solutions of the model correspond to two orthogonal linearly polarized states, referred to as x and y . In certain parameter regions, solutions corresponding to elliptically polarized states also exist [16]. The stability of these solutions determine the polarization of the emitted light. The variation of a parameter, typically the pump current, can result in a change of stability, which in turn can result in a switching from one polarization state to the orthogonal one, a phenomenon known as polarization switching (PS). When scanning the pump current upwards and downwards the PSs occur at different current values, which define the boundaries of a polarization bistable region, as shown in Fig. 1(a), that displays the polarization resolved light-output characteristic. These boundaries depend, among other parameters, on the noise strength and on the speed of the variation of the pump current [19, 20].

Near the PS points, stochastic, i.e. noise-induced, switching can also occur. It has been shown that, in spite of the potentially complicated polarization dynamics, key features of the PS (such

as the distribution of residence times in each polarization state) can be well understood as stochastic hopping in an effective 1D double-well potential [17].

Figure 1(b) displays schematically the effective potential associated to the polarization switching scenario shown in Fig. 1(a). In the low current region [labeled I in Fig. 1(a)] the laser can only emit the y polarization. The effective potential has only one well [potential labeled I in Fig. 1(b)]. For increasing pump there is a region of pump current values [labeled II in Fig. 1(a)] where there is bistability and there is a small probability of emission of the x polarization. The effective potential, labeled II in Fig. 1(b), is a double-well potential, with a small right well. In this region of pump current values, if the laser emits the x polarization, a weak perturbation or a small amount of noise has a large probability to trigger a PS to the y polarization; but on the contrary, if the laser emits the y polarization, there is only a small probability that a fluctuation will trigger a PS. As the pump increases the switching probabilities vary and at the right boundary of the bistable region [label III in Fig. 1(a)] the most probable polarization is the x polarization. If the laser emits the y polarization, a weak perturbation or a small amount of noise can trigger a switch to the x polarization. In this region the effective potential is the double-well potential labeled III in Fig. 1(b), which has a small left well. Finally, for high pump current [region label IV in Fig. 1(a)], the laser emits the x polarization and the effective potential has only one well [potential labeled IV in Fig. 1(b)].

It is important to remark that the polarization-resolved light-output characteristic, displayed in Fig. 1(a), represents the laser *quasi-static* polarization response, as the injection current was varied very slowly compared to the laser characteristic time scales. Therefore, the boundaries of the quasi-static polarization bistability region, and the associated 1D effective potentials, will be a good representation of the *dynamic* polarization response only at low modulation frequencies, and will fail to describe the laser polarization at high frequencies [18–20]. To illustrate how the polarization bistability region changes when the variation of the bias current is fast, Fig. 1(c) displays the polarization resolved light-output characteristic [the same as Fig. 1(a)], but now μ varies much faster. It can be noticed that the threshold is at a higher value of μ , the laser turns on with relaxation oscillations, the PS for decreasing current disappears (the x polarization remains on until the laser turns off) and the size of the bistability region increases.

3. Stochastic logic gate implemented via direct modulation of the pump current

In this section we analyze how two logic inputs can be encoded in a three-level aperiodic modulation directly applied to the laser pump current, and how to define the laser logical response.

Let's consider that the pump current parameter, $\mu(t)$, is the sum of two aperiodic square-waves, $\mu(t) = \mu_1(t) + \mu_2(t)$, that encode the two logic inputs. Since the logic inputs can be either 0 or 1, we have four distinct input sets: (0, 0), (0, 1), (1, 0), and (1, 1). Sets (0, 1) and (1, 0) give the same value of μ , and thus, the four distinct logic sets reduce to three μ values. Then, it is more convenient to introduce as parameters the mean value, μ_0 , and the amplitude of the modulation, $\Delta\mu$, which, without loss of generality, determine the three current levels as $\mu_0 - \Delta\mu$, μ_0 , and $\mu_0 + \Delta\mu$.

The laser response is determined by the polarization of the emitted light. We chose parameters such that the laser emits either the x or the y polarization (parameter regions where there is anti-correlated polarization coexistence or elliptically polarized light are avoided). The laser response is considered a logical 1 if, for instance, the x polarization is emitted, and a logical 0, if the y polarization is emitted. Which polarization represents a logic 1, and which a logic 0 can depend on the logic operation, as will be discussed latter.

In this way, the polarization emitted at the three current levels, encoding the four possible combinations of the two logic inputs, allows to implement the operations OR, AND, NOR, NAND, according to Table 1. One should notice that by detecting one polarization one obtains

a logic response and, by detecting the orthogonal polarization, one obtains the negation of that logic response. In the following we focus only on the non-negation operations AND and OR.

Table 1. Relationship between the two inputs and the output of the logic operations.

Logic inputs	AND	NAND	OR	NOR
(0,0)	0	1	0	1
(1,0)/(0,1)	0	1	1	0
(1,1)	1	0	1	0

There are two ways to associate the four possible logic inputs, (0,0), (1,0), (0,1), (1,1), to three current levels. The first one is schematically illustrated in Fig. 1(b). In the presence of a right amount of noise, the levels μ_I , μ_{II} , μ_{III} can lead to the operation AND, and levels μ_{II} , μ_{III} , μ_{IV} , to the operation OR.

Let's explain the idea by first considering the operation AND. Assuming that x represents a logical 1 and y represents a logical 0, and assuming that the laser is emitting the y polarization, only the current level μ_{III} [representing the logic input (1,1)] will induce a switch to the x polarization; however, the probability of this switch will be controlled by the noise strength.

Let's now consider the operation OR: if the laser is emitting the y polarization, the current levels μ_{III} and μ_{IV} [representing the inputs (0,1), (1,0) and (1,1)] will both induce a switch to the x polarization. The main idea behind LSR is that the current levels can be chosen such that the probability of the switchings is controlled by the noise strength.

Table 2 summarizes the relationship between the logic inputs, the current levels encoding these inputs, the expected laser polarization and its associated logical output.

A main advantage of this scheme is that it allows to switch from AND to OR and vice versa, just by changing the cw value of the injection current, μ_0 , while the modulation amplitude, $\Delta\mu$, can be kept constant. In other words, an appropriate choice of $\Delta\mu$, allows switching from regions (I, II, III) represented schematically in Fig. 1(a), that implement the AND operation, to regions (II, III, IV), that implement the OR operation, by changing μ_0 only. A main drawback is that, for the AND operation, it does not allow very fast modulation. This is due to the fact that, as discussed previously in relation to Fig. 1(c), under fast modulation the PS for decreasing injection current disappears, and thus, there might be no level μ_I for which the y polarization turns on when the current decreases from levels μ_{II} or μ_{III} to μ_I .

Table 2. Encoding scheme I: Relationship between the logic inputs, the encoding current levels, the output polarization and the logic output for the AND and OR operations.

Logic inputs	AND:			OR:		
	Current	Polarization	Logic output	Current	Polarization	Logic output
(0,0)	μ_I	y	0	μ_{II}	y	0
(1,0)/(0,1)	μ_{II}	y	0	μ_{III}	x	1
(1,1)	μ_{III}	x	1	μ_{IV}	x	1

Table 3 illustrates the second encoding possibility. Here the current levels employed for the AND and for the OR operation are the same (they are those described for the OR operation previously). It should be noticed that for the AND operation the definition of the laser logic response changes: now is a logic 0 if the x polarization is emitted, and a logic 1 if the y polarization is emitted. Also the encoding criterium changes, in the sense that the lower current level μ_{II} encodes the input (0, 0) for the OR operation, while it encodes the input (1, 1) for the AND operation; the highest current level μ_{IV} encodes the input (1, 1) for OR and encodes

Table 3. Encoding scheme II: Relationship between the logic inputs, the encoding current levels, the output polarization and the logic output for the AND and OR operations.

Logic inputs	AND:			OR:		
	Current	Polarization	Logic output	Current	Polarization	Logic output
(0,0)	μ_{IV}	x	0	μ_{II}	y	0
(1,0)/(0,1)	μ_{III}	x	0	μ_{III}	x	1
(1,1)	μ_{II}	y	1	μ_{IV}	x	1

(0, 0) for AND; the middle level μ_{III} encodes (1,0) and (0, 1) for both operations. Because the AND and OR operations are implemented with the same three current levels, this scheme has the advantage of allowing fast modulation in both, AND and OR operations.

In the following we will focus on the OR operation as the results apply also for the symmetric AND operation implemented with the second encoding scheme, described in Table 3.

The shape of the three-level signal directly applied to the laser pump current is shown in Fig. 1(d): within each modulation bit, the current is constant during a time interval T_1 , referred to as the step time, then, there is a ramp (up or down) to the current level encoding the next bit. The time required for the signal to change from one value to the next (the rise time or the fall time depending on the bit sequence), T_2 , is such that $T_2 \ll T_1$. Each bit begins at the middle of one ramp and finishes at the middle of the next one, as indicated in Fig. 1(d), and thus the length of the bit is $T = T_1 + T_2$. As will be discussed in the next section, the value of T_1 strongly influences the reliability of the VCSEL logic gate, but the value of T_2 does not affect significantly the operation, as long as $T_2 \ll T_1$.

4. Results

The model equations were simulated with the following parameters: $k = 300 \text{ ns}^{-1}$, $\alpha = 3$, $\gamma_N = 1 \text{ ns}^{-1}$, $\gamma_a = 0.5 \text{ ns}^{-1}$, $\gamma_p = 50 \text{ rad ns}^{-1}$ and $\gamma_s = 50 \text{ ns}^{-1}$. As explained before, we chose these parameters not only because they are typically used in the literature [16], but also, because there is no polarization coexistence or elliptically polarized light, i.e., the laser emits either the x or the y polarization, and the PS from one polarization to the orthogonal one is rather abrupt. As will be discussed later, the operation of the VCSEL-based stochastic logic gate is robust and does not require fine tuning of the parameters. In the following we focus on the logic OR operation and, unless otherwise specifically stated, we use the following parameters for the three-level aperiodic signal: $\mu_0 = 1.3$, $\Delta\mu = 0.27$, $T = T_1 + T_2 = 31.5 \text{ ns}$, $T_1 = 31 \text{ ns}$, and $T_2 = 0.5 \text{ ns}$. When the time duration of the bit T is varied, T_1 and T_2 are varied such that their ratio is kept constant.

Figures 2(a)–2(c) display the laser response for the same logic input and three values of the noise strength. The three current levels are such that the laser emits one polarization (x) for two of them, while for the third one, it can switch to the orthogonal polarization (y), in the presence of the right amount of noise. Figures 2(d)–2(f) display a detail of the dynamics to show the effects of the noise and the current modulation in the PS. With weak noise the PS is delayed with respect to the current modulation [Fig. 2(d)]; with too strong noise, both polarizations are emitted simultaneously within the same bit [Fig. 2(f)]. Therefore, the operation of the VCSEL as a logic gate depends on the noise strength, in good agreement with Ref. [13].

5. Analysis of the reliability of the VCSEL logic gate

To evaluate the reliability of the VCSEL-based logic gate we calculate the success probability, i.e., the probability to obtain the desired logic output. For the two logic inputs we generate two

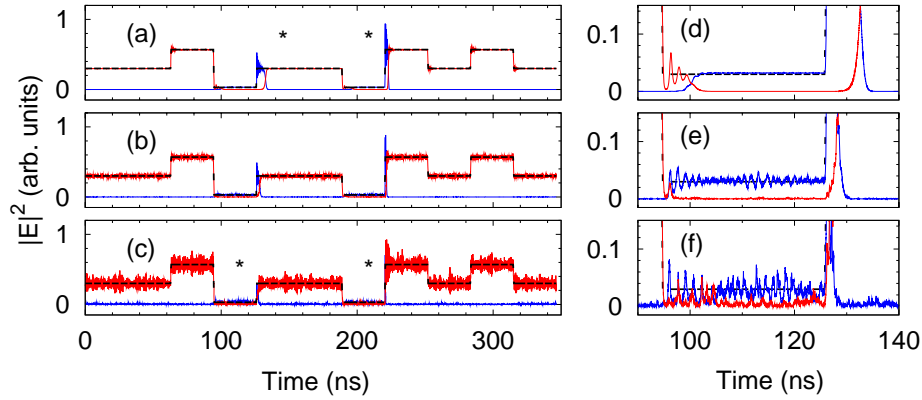


Fig. 2. Time traces of the x polarization (solid red), y polarization (solid blue), and the injection current $\mu - 1$ (dashed black) for different noise intensities: (a), (d) $D = 5 \times 10^{-7} \text{ ns}^{-1}$, (b), (e) $D = 4 \times 10^{-4} \text{ ns}^{-1}$ and (c), (f) $D = 6 \times 10^{-3} \text{ ns}^{-1}$. (d)-(f) display a detail of (a)-(c) to show the main errors in a bit. The asterisks mark the wrong bits. The parameters are: $T = 31.5 \text{ ns}$, $\mu_0 = 1.3$, $\Delta\mu = 0.27$, $k = 300 \text{ ns}^{-1}$, $\alpha = 3$, $\gamma_N = 1 \text{ ns}^{-1}$, $\gamma_a = 0.5 \text{ ns}^{-1}$, $\gamma_p = 50 \text{ rad ns}^{-1}$ and $\gamma_s = 50 \text{ ns}^{-1}$.

random uncorrelated sequences of N bits and compute the success probability, P , as the ratio between the number of correct bits to the total number of bits. In the following, $N \geq 2^{10}$. We define that a bit is correct, as follows. When x is the “right” output polarization, we count a bit as correct if a given percentage (say, 80%) or more of the emitted power is emitted in the x polarization; if x is the “wrong” polarization, we count a bit as correct if a given percentage (say, 20%) or less of the emitted power is emitted in the x polarization.

Figure 3(a) displays P as a function of the noise strength, for three success criteria: 80%-20%, 90%-10% and 70%-30%. One can notice that there is a range of noise strengths in which $P = 1$, and this noise range decreases (increases) when choosing a restrictive (a permissive) threshold for the emitted power in the x polarization. Within this noise range there is optimal noise-activated polarization switchings (the “inter-well” dynamics in the double-well potential picture) and optimal sensitivity to spontaneous emission in each polarization (the “intra-well” dynamics in the double-well potential picture). In the following we fix the success criterium to 80%-20%. It should be noticed that $P = 1$ occurs for noise strengths D that do not have to be unusually small, on the contrary, they are realistic values for semiconductor lasers, which typically have $\beta_{sp} \sim 10^{-4}$.

The success probability depends strongly on the bit time, T , as shown in Fig. 3(b). Short bits ($\lesssim 5 \text{ ns}$) prevent logical operations because of the finite time need for the polarization switching. For increasing T , the success probability grows monotonically until it saturates at $P = 1$ for long enough bits, for which the PS time is $\ll T$.

The interplay between the duration of the bit and the noise strength is illustrated in Fig. 3(c) and can be interpreted as follows. The time needed to escape from a potential well decreases with increasing noise [21]. Then, for weak noise, as D increases the escape time decreases and the probability of a correct response grows. On the other hand, too strong noise results in spontaneous emission in both polarizations and thus, for large enough noise, the power emitted in the “wrong” polarization grows above the threshold for detecting the response as correct, and thus, above a certain noise level the success probability decreases monotonously. The dependence of the success probability on the noise strength is due to the interplay of noise-induced

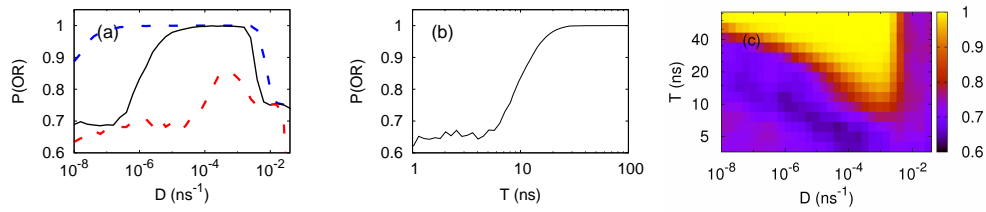


Fig. 3. (a) Success probability P as a function of the noise strength, D , keeping fixed the bit time $T = 31.5$ ns and using a success criterium of 80%-20% (black solid line), 90%-10% (red dashed line) and 70%-30% (blue dashed line), see text for details. (b) Success probability as a function of the bit time T for fixed noise strength $D = 4 \times 10^{-4}$ ns $^{-1}$. (c) Log-log color plot of the success probability P as a function of the noise intensity, D , and the bit time, T . Other parameters as in Fig. 2.

escapes (inter-well stochastic dynamics) and spontaneous emission noise in the two polarizations (intra-well stochastic dynamics).

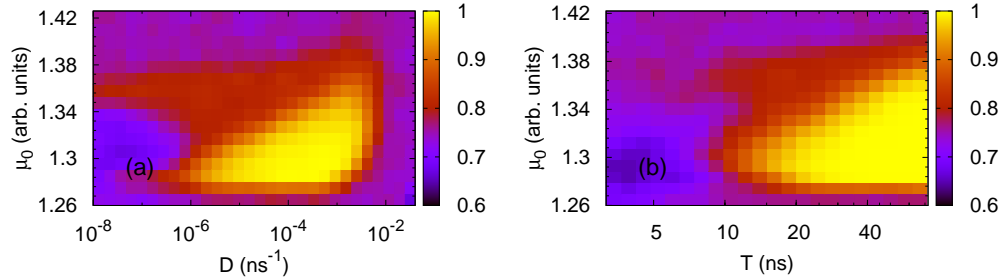


Fig. 4. (a) Color plot of the success probability P as a function of the noise intensity, D , and the cw current value, μ_0 , for fixed bit length $T = 31.5$ ns and modulation amplitude $\Delta\mu = 0.27$. (b) Color plot of the success probability P as a function of the bit time, T , and the cw current value, μ_0 for fixed noise strength $D = 4 \times 10^{-4}$ ns $^{-1}$ and modulation amplitude $\Delta\mu = 0.27$. Other parameters are as in Fig. 2.

Figure 4(a) displays the success probability in the plane (D, μ_0) , for constant bit length and modulation amplitude. It can be seen that for small μ_0 logic operations can not be obtained for any noise strength. Above $\mu_0 \sim 1.27$, there is a noise range in which P suddenly grows to 1. This value of μ_0 is such that $\mu_{II} \geq \mu_{th,s} = 1$, i. e. the lasing threshold. As μ_0 increases the noise region where $P = 1$ decreases until it disappears, due to the fact that for large μ_0 the x polarization is stable in the three current levels, and switches to the y polarization are rare.

Figure 4(b) displays the success probability in the (T, μ_0) plane, keeping fixed the noise strength and modulation amplitude. It can be seen that $P = 1$ occurs when T is long enough and μ_0 is within a range of values that depends on T . As discussed in relation to Fig. 4(a), if μ_0 is too small the current level μ_{II} is at the lasing threshold or below and the y polarization turns-on slowly or does not turn on at all, depending on the modulation speed (if T is too small the y polarization does not turn on); on the other hand, if μ_0 is too large, then the x polarization is stable in the three current levels and the y polarization rarely turns on.

Next, let us consider the influence of the modulation amplitude, $\Delta\mu$. Figure 5(a) displays the success probability in the $(D, \Delta\mu)$ plane, keeping constant the bit length and the modulation

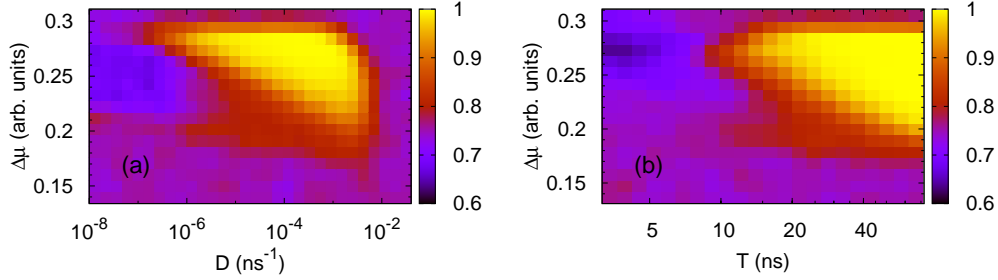


Fig. 5. Color plot of the success probability P (a) as a function of the noise strength, D , and the current modulation amplitude, $\Delta\mu$, for a fixed $T = 31.5$ ns and (b) as a function of the bit time, T , and the current modulation amplitude, $\Delta\mu$, for a fixed $D = 4 \times 10^{-4}$ ns $^{-1}$. Other parameters are as in Fig. 2.

cw value. If $\Delta\mu$ is small the laser emits the same polarization in the three current levels and the success probability is small, regardless of the noise strength. As $\Delta\mu$ increases there are polarization switchings and P increases, allowing for the correct logic response in a finite range of noise strengths. For large $\Delta\mu$, P decreases abruptly to small values, and this is again because the lowest current level is at threshold or below threshold [one can notice the similarities between Figs. 4(a) and 5(a)]. Similar considerations can be done in relation to Fig. 5(b), that displays the success probability in the $(T, \Delta\mu)$ plane, keeping constant the noise strength and the modulation cw value.

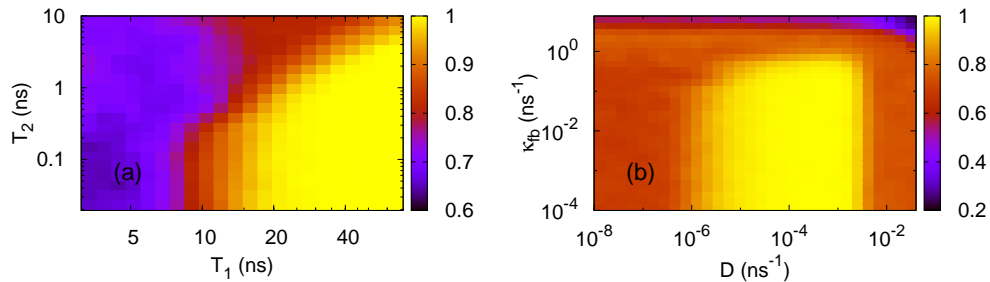


Fig. 6. (a) Color plot of the success probability P as a function of the step time, T_1 , and the rise/fall time, T_2 , the noise level is $D = 4 \times 10^{-4}$ ns $^{-1}$ and other parameters are as in Fig. 2. (b) P as a function of the noise strength, D , and the feedback strength, κ_{fb} . The bit time is $T = 31.5$ ns, the time delay is 3 ns and other parameters are as in Fig. 2.

The step time, T_1 , and the rise/fall time, T_2 , are important parameters to obtain a correct logic response. In Fig. 6(a) we show the probability of success as a function of T_1 and T_2 . $P = 1$ requires that $T_1 \gg T_2$ (notice the vertical logarithmic scale). Furthermore, exist a minimum value of $T_1 \sim 10$ ns above which the probability of success grows to 1.

In practical applications, a VCSEL is often submitted to unwanted optical feedback due to external reflections. If the laser is sensitive enough, even a weak amount of reflected light can induce instabilities. To test the reliability of the LSR under the influence of a weak external reflection, we included optical isotropic feedback in the model equations as in [22], and in

Fig. 6(b) we present the results. By plotting the success probability in the parameter space (feedback strength, noise strength) we can see that the logic response is robust for weak feedback but the optimal response decreases progressively for increasing feedback strength.

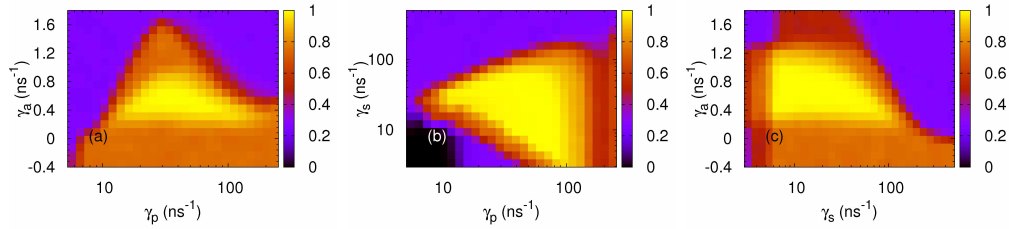


Fig. 7. Influence of various model parameters. (a) Success probability in parameter plane (γ_a, γ_p) , for $\gamma_s = 50 \text{ ns}^{-1}$; (b) P in the parameter plane (γ_s, γ_p) , for $\gamma_a = 0.5 \text{ ns}^{-1}$; P in the parameter plane (γ_a, γ_s) , for $\gamma_p = 50 \text{ rad ns}^{-1}$. Other parameters are as in Fig. 2.

We conclude this section with a discussion of the influence of various laser parameters. As it was previously mentioned, the logic stochastic resonance is a robust phenomenon in the sense that it occurs in parameter regions where the polarization switching is abrupt, and does not display polarization oscillations or coexistence. Figure 7(a) displays the success probability in the plane (γ_p, γ_a) . For negative or low linear dichroism, γ_a , only the x polarization is emitted. A probability equal to 1 is achieved in a region of positive γ_a values, and in a broad range of birefringence values, γ_p . Figure 7(b) displays the success probability in the plane (γ_s, γ_p) , and it can be seen that there is a wide region in which the success probability is equal to 1, provided that $\gamma_s \leq 100$. For large spin-flip rate, γ_s , only the polarization y is emitted and for small γ_s both polarizations are emitted simultaneously. Finally, Fig. 7(c) displays the success probability in the plane (γ_s, γ_a) where also a parameter region can be seen where $P = 1$.

6. Discussion and conclusion

To conclude, we have shown that a VCSEL can operate as a logic gate with a success probability equal to 1 in a wide region of noise strengths, which makes the VCSEL logic gate attractive for applications in systems subjected to noisy backgrounds.

The phenomenon is based on logic stochastic resonance (LSR) and can be well understood in the framework of the simple effective double well potential model for the two orthogonal polarizations emitted by the laser in a certain range of injection currents. The three levels of the pump current aperiodic signal that encode the four possible combinations of the two logic inputs are chosen such that the laser emits one polarization for two of them, while for the third one, it can switch to the orthogonal polarization, in the presence of the right amount of noise. Thus, the successful operation of a VCSEL as an stochastic logic gate is associated with optimal noise-activated polarization switchings (the “inter-well” dynamics) and optimal sensitivity to spontaneous emission in each polarization (the “intra-well” dynamics) leading a range of optimal noise strength.

Our study has been based on the “bare” spin-flip model, which does not take into account several mechanisms that could be very relevant for the efficiency of current modulation to induce polarization switching (e.g., thermal effects, the excitation of higher-order transverse modes, carrier diffusion, etc. [23, 24]). The spin-flip model was recently extended to take into account temperature variations [25], and the study of the interplay of temperature and transverse spatial effects, based on the extended spin-flip model, is a natural continuation of the present work, that is left for future work. We think that these effects will not change the main conclusions of

this work, but, since thermal effects are slow, they will probably increase the minimum bit time needed for achieving successful polarization switchings.

The mechanism underlying LSR has some similarities with that proposed in Ref. [26] for localizing a Brownian particle in one well of a symmetric bistable potential through the simultaneous action of two periodic inputs (one tilting the minima and the other one modulating the barrier height), and a random input. In Ref. [26] it was shown that the nonlinear mixing of these zero-mean signals was capable of localizing a Brownian particle in one well, and this could be a mechanism for controlling the polarization state of the light emitted by a VCSEL.

LSR also resembles the aperiodic stochastic resonance phenomenon, by which there is noise-assisted transmission of binary information [27, 28], and the information transmission, measured by the bit-error rate, exhibits a resonant-like behavior as a function of the noise strength.

The constructive role of noise in optical systems is nowadays a hot topic of research. Nonlinear self-filtering and amplification of noisy images, the with amplification occurring at the expense of noise through nonlinear coupling, was recently demonstrated in a self-focusing photorefractive medium [29]. The underlying mechanism (the energy exchange between the signal and the noise via nonlinear mixing), depends on the system parameters and thus noise-assisted image recovery represents a novel type of dynamical stochastic resonance.

Our proposed implementation of a stochastic logic gate via a polarization-bistable VCSEL thus provides yet another example of the nontrivial and constructive role of noise in nonlinear optical systems. An attractive advantage of the VCSEL stochastic logic gate for practical applications is the relatively short bit time needed to produce the correct operation with probability equal to 1 (in our simulations, about 30-40 ns). In addition, the VCSEL stochastic logic gate is robust to stochastic external perturbations, in the sense that there is a wide range of realistic noise strengths in which the device gives a reliable and correct logic response. Moreover, its operation is also robust to variations of the laser parameters, in the sense that it does not require fine tuning of the parameters, but rather, there is a wide region of parameter values where the laser gives the correct logic response with $P = 1$.

Acknowledgment

This research was supported by AFOSR grant FA-8655-10-1-3075, the Spanish Ministerio de Educacion y Ciencia through Grants FIS2008-06024-C03-02 and FIS2009-13360-C03-02 and the Agència de Gestió d'Ajuts Universitaris i de Recerca, Generalitat de Catalunya through Grant 2009 SGR 1168.